$Sb_2F_{11}^-$, 39797-64-3; $XeO_2F^+Sb_2F_{11}^-$, 52078-91-8; $XeOF_4$, 13774-85-1; SbF_5, 7783-70-2; IOF_3, 19058-78-7; XeO_2F_2, 13875-06-4.

References and Notes

(1) N. Bartlett and F. O. Sladky, "Comprehensive Inorganic Chemistry", Vol. 1, J. C. Bailar and A. F. Trotman-Dickenson, Ed., Pergamon Press, Oxford, 1973 Chaper 6.
(2) R. J. Gillespie and B. Landa, *Inorg. Chem.*, **12**, 1383 (1973).
(3) R. J. Gillespie, A. Netzer, and G. J. Schrobilgen, *Inorg. Chem.*, **13**, 1455 (1974).
(4) V. M. McRae, R. D. Peacock, and D. R. Russell, *Chem. Commun.*, 62 (1969).
(5) N. Bartlett, M. Gennis, D. D. Gibler, B. K. Morrell, and A. Zalkin, *Inorg. Chem.*, **12**, 1717 (1973).
(6) N. Bartlett, F. Einstein, D. F. Stewart, and J. Trotter, *J. Chem. Soc.*, **4**, 1190 (1967).
(7) N. Bartlett, B. G. De Boer, F. J. Hollander, F. O. Sladky, D. H. Templeton, and A. Zalkin, *Inorg. Chem.*, **13**, 780 (1974).
(8) K. Leary, D. H. Templeton, A. Zalkin, and N. Bartlett, *Inorg. Chem.*, **12**, 1726 (1973).
(9) R. J. Gillespie and G. J. Schrobilgen, *Inorg. Chem.*, **13**, 765 (1974).
(10) B. Landa and R. J. Gillespie, *Inorg. Chem.*, in press.
(11) K. O. Christe, E. C. Curtis, and R. D. Wilson, private communication.
(12) D. E. McKee, C. J. Adams, A. Zalkin, and N. Bartlett, *J. Chem. Soc., Chem. Commun.*, 26 (1973).
(13) N. Bartlett and M. Wechsberg, *Z. Anorg. Allg. Chem.*, **385**, 5 (1971).
(14) B. Frlec, M. Bolinc, P. Charpin, and M. Drifford, *J. Inorg. Nucl. Chem.*, **34**, 2938 (1972).
(15) F. O. Sladky, P. A. Bulliner, N. Bartlett, B. G. DeBoer, and A. Zalkin, *Chem. Commun.*, 1048 (1968).
(16) K. Leary, A. Zalkin, and N. Bartlett, *J. Chem. Soc., Chem. Commun.*, 131 (1973).
(17) K. Leary, A. Zalkin, and N. Bartlett, *Inorg. Chem.*, **13**, 775 (1974).
(18) N. Bartlett and F. O. Sladky, *J. Am. Chem. Soc.*, **90**, 5316 (1968).
(19) D. Gibler, B. Morrell, N. Bartlett, and A. Zalkin, Abstracts, 162d National Meeting of the American Chemical Society, Washington, D.C., Sept 13–17, 1971, No FLUO 1.
(20) (a) B. Cohen and R. D. Peacock, *J. Inorg. Nucl. Chem.*, **28**, 3056 (1966); (b) D. Martin, *C. R. Hebd. Seances Acad. Sci., Ser. C*, 1145 (1969).
(21) H. Selig, *Inorg. Chem.*, **5**, 183 (1966).
(22) R. J. Gillespie, B. Landa, and G. J. Schrobilgen, *Chem. Commun.*, 1515 (1971).
(23) R. J. Gillespie, B. Landa, and G. J. Schrobilgen, *J. Chem. Soc., Chem. Commun.*, 607 (1972).
(24) P. Boldrini, R. J. Gillespie, P. R. Ireland, and G. J. Schrobilgen, *Inorg. Chem.*, **13**, 1690 (1974).
(25) R. J. Gillespie and G. J. Schrobilgen, *Inorg. Chem.*, **13**, 2370 (1974).
(26) D. E. McKee, A. Zalkin, and N. Bartlett, *Inorg. Chem.*, **12**, 1713 (1973).
(27) D. E. McKee, C. J. Adams, and N. Bartlett, *Inorg. Chem.*, **12**, 1722 (1973).
(28) H. Selig, H. H. Claassen, and J. H. Holloway, *J. Chem. Phys.*, **52**, 3517 (1970).
(29) H. Schmeisser, D. Naumann, and E. Lehmann, *J. Fluorine Chem.*, **3**, 441 (1973).
(30) H. H. Hyman, "Physical Chemistry", Vol. 5, H. Eyring, D. Henderson, and W. Jost, Ed., Academic Press, New York, N.Y., 1970 Chapter 11, p 610.
(31) See ref 30, pp 611–612
(32) R. J. Gillespie, "Molecular Geometry", Van Nostrand-Reinhold, London, 1972.
(33) R. J. Gillespie and G. J. Schrobilgen, *Inorg. Chem.*, **15**, 22 (1976).
(34) R. L. Carter, *J. Chem. Educ.*, **48**, 297 (1971).
(35) W. G. Fateley, F. R. Dollish, N. T. McDevitt, and F. F. Bentley, "Infrared and Raman Selection Rules for Molecular and Lattice Vibrations: The Correlation Method", Wiley-Interscience, New York, N.Y., 1972.
(36) P. A. W. Dean, R. J. Gillespie, and R. Hulme, *Chem. Commun.*, 990 (1969).
(37) K. O. Christe and E. C. Curtis, *Inorg. Chem.*, **11**, 2196 (1972).
(38) G. M. Begun, W. H. Fletcher, and D. F. Smith, *J. Chem. Phys.*, **42**, 1229 (1965).
(39) H. H. Claassen and G. Knapp, *J. Am. Chem. Soc.*, **86**, 2341 (1964).
(40) K. Nakamoto, "Infrared Spectra of Inorganic and Coordination Compounds", 2d ed, Wiley-Interscience, New York, N.Y., 1970.
(41) R. J. Gillespie and P. Spekkens, *J. Chem. Soc., Chem. Commun.*, 314 (1975).
(42) H. A. Carter and F. Aubke, *Inorg. Chem.*, **10**, 2296 (1971).
(43) J. G. Malm and C. L. Chernick, *Inorg. Synth.*, **8**, 254, 258 (1966).
(44) I. Sheft, T. M. Spittler, and F. H. Martin, *Science*, **145**, 701 (1964).
(45) C. L. Chernick, H. H. Claassen, T. G. Malm, and P. F. Plurien in "Noble Gas Compounds", H. H. Hyman, Ed., University of Chicago Press, Chigaco, Ill., 1963, p 106.

Contribution from the Department of Chemistry,
The University of Leicester, Leicester LE1 7RH, England

Preparation and Characterization of $2KrF_2 \cdot SbF_5$, $KrF_2 \cdot MF_5$ (M = Sb, Ta), and $KrF_2 \cdot 2MF_5$ (M = Sb, Ta, Nb): the $[Kr_2F_3]^+$ and $[KrF]^+$ Cations[1]

BORIS FRLEC[2] and JOHN H. HOLLOWAY*

Received May 20, 1975

AIC503529

The new adducts $2KrF_2 \cdot SbF_5$, $KrF_2 \cdot MF_5$ (M = Sb, Ta), and $KrF_2 \cdot 2MF_5$ (M = Ta, Nb) have been prepared and characterized, and $2KrF_2 \cdot TaF_5$ has been obtained in solution. Raman spectra of these adducts and the already known $KrF_2 \cdot 2SbF_5$ are interpreted in terms of the molecules having fluorine-bridged (Kr···F···M) contributions to the bonding as well as contributions from ionic formulations such as $[Kr_2F_3]^+[MF_6]^-$ and $[KrF]^+[MF_6]^-$ (M = Sb, Ta) and $[KrF]^+[M_2F_{11}]^-$ (M = Sb, Ta, Nb). Thermal decomposition studies on some of the adducts have produced evidence for other new adducts which can be conveniently formulated as $[xKrF_2 \cdot KrF]^+[Ta_2F_{11}]^-$ and $[xKrF_2 \cdot KrF]^+[Nb_2F_{11}]^-$ (where x is probably equal to 1), in which the additional KrF_2 units appear to be weakly associated with the cationic parts of the adducts.

Introduction

The difficulty in preparing large-scale samples of KrF_2 and the fact that the compound is said to decompose readily at room temperature[3] has impeded progress with its chemistry. Until our own[1] and Gillespie and Schrobilgen's recent work[4] the only established krypton compound, other than KrF_2 itself, was $KrF_2 \cdot 2SbF_5$.[5a] This has recently been characterized by Bartlett and his co-workers as the salt $[KrF]^+[Sb_2F_{11}]^-$.[5b]

Other information on krypton difluoride chemistry has been published by Russian workers.[6,7] In an extensive review on krypton difluoride they briefly mentioned krypton difluoride adducts of the types $KrF_2 \cdot MF_5$ (M = Sb, Ta), $KrF_2 \cdot 2MF_5$ (M = Sb, Ta, Nb), and $2KrF_2 \cdot MF_4$ (M = Ti, Sn) but no details of preparation or characterization were reported.[6] In another paper, however, the same authors claimed that $KrF_2 \cdot 2SbF_5$ is the only compound formed in the KrF_2–SbF_5–BrF_5 system.[7]

We have investigated the reactions of KrF_2 with NbF_5, TaF_5, and $[BrF_4]^+[Sb_2F_{11}]^-$ in BrF_5 solution and the thermal decompositions of the materials which can be separated. The solid adducts $2KrF_2 \cdot SbF_5$, $KrF_2 \cdot MF_5$ (M = Sb, Ta), and $KrF_2 \cdot 2MF_5$ (M = Ta, Nb) have been prepared and characterized by gravimetry and Raman spectroscopy for the first time and evidence for $2KrF_2 \cdot TaF_5$ has been observed in solution. The Raman spectrum of $KrF_2{\cdot}2SbF_5$ has also been recorded and assigned. X-ray powder photographic and infrared spectroscopic examination of some of the compounds has been made. We have shown that the main Raman shifts in solid $2KrF_2{\cdot}SbF_5$ and related shifts in the spectra of mixtures of excess of KrF_2 with TaF_5 in BrF_5 solution can be assigned to $[Kr_2F_3]^+$ stretching modes. As first pointed out by Gillespie and Schrobilgen,[4] this cation appears to have an asymmetric fluorine-bridged structure unlike its xenon analogue.[8] The strongest bands in the Raman spectra of $KrF_2{\cdot}MF_5$ (M = Sb, Ta) and $KrF_2{\cdot}2MF_5$ (M = Ta, Nb) can be assigned to $\nu(Kr{-}F^+)$ split by weak intermolecular coupling. These frequencies, together with those associated with $\nu(Kr{-}F^+)$ in $KrF_2{\cdot}2SbF_5$, decrease in the order $SbF_5 > TaF_5 > NbF_5$ for both series of adducts in a way similar to that of their xenon difluoride analogues.[9] This we have interpreted as indicative of a progressive lengthening of the Kr–F bond in KrF^+ and an increasing contribution to the bonding from the fluorine-bridged structures $F{-}Kr{\cdots}F{-}MF_5$ or $F{-}Kr{\cdots}F{-}M_2F_{10}$.

Thermal decomposition studies on the adducts containing the highest KrF_2 content have produced evidence for other new adducts which contain weakly associated KrF_2. These can be conveniently formulated as $[xKrF_2{\cdot}KrF]^+[Ta_2F_{11}]^-$ and $[xKrF_2{\cdot}KrF]^+[Nb_2F_{11}]^-$ (where x is probably equal to 1).

Results and Discussion

Preparations of the Antimony Pentafluoride Adducts. The direct reaction of KrF_2 with SbF_5 at room temperature takes place even in the vapor phase and the exothermicity of the reaction results in the decomposition of a substantial portion of KrF_2 and the product. In some experiments white and blue flames accompanied the decompositions. Reaction of the decomposing KrF_2 with the Kel-F or glass walls of the reactor also occurs. The Raman spectra of solids resulting from such reactions, where the initial ratio of the components is $KrF_2{:}SbF_5 = {\sim}3{:}1$, indicate the formation of mixtures of mainly $KrF_2{\cdot}SbF_5$ and $KrF_2{\cdot}2SbF_5$.

The reaction of KrF_2 with solid $[BrF_4]^+[Sb_2F_{11}]^-$ at room temperature gives BrF_5 and the corresponding reaction in BrF_5 solution results in the total decomposition of KrF_2 to krypton and fluorine. At −40 °C, however, a rather slow reaction occurs and, provided an excess of krypton difluoride is used, $2KrF_2{\cdot}SbF_5$ is produced in the solution (solubility at −40 °C is ~0.15 mmol/100 g of solvent). The solvent and excess of KrF_2 can be removed at −50 °C to leave a white solid. The weight loss vs. time of pumping curve at this temperature levels out close to the weight expected for the composition $2KrF_2{\cdot}SbF_5$. The solid is quite stable at −40 °C in a dynamic vacuum but slowly decomposes at −30 °C to give KrF_2 and $KrF_2{\cdot}SbF_5$.

When the reaction is carried out with a $KrF_2{:}SbF_5$ (from $[BrF_4]^+[Sb_2F_{11}]^-$) ratio approaching 2:1, the product is more heavily contaminated with $[KrF]^+[SbF_6]^-$ than in reactions where larger excesses of KrF_2 are used. Figure 1 shows a weight loss vs. time of pumping curve for the product from a reaction of 4.14 mmol of KrF_2 with 2.02 mmol of SbF_5 in BrF_5. The complexity of initial product is reflected in the poor correlation of the first point of inflection with the expected weight of $2KrF_2{\cdot}SbF_5$. However, there is close agreement with the expected weight loss after further decomposition to the more stable $KrF_2{\cdot}SbF_5$.

$KrF_2{\cdot}SbF_5$ is stable at room temperature in a dynamic vacuum. Its x-ray powder diffraction pattern shows a very close relationship to that of $XeF_2{\cdot}TaF_5$ (or the isostructural $XeF_2{\cdot}NbF_5$)[9] but there is a more marked difference between that of $KrF_2{\cdot}SbF_5$ and its xenon analogue.[9] The solid melts at 45 ± 1 °C with decomposition. Above 35 °C under a dynamic vacuum it slowly decomposes to give the more stable, cream-colored $KrF_2{\cdot}2SbF_5$ and KrF_2, some of which is decomposed into krypton and fluorine. The adduct $KrF_2{\cdot}2SbF_5$, like the 1:1 adduct, is stable under a dynamic vacuum at room temperature.

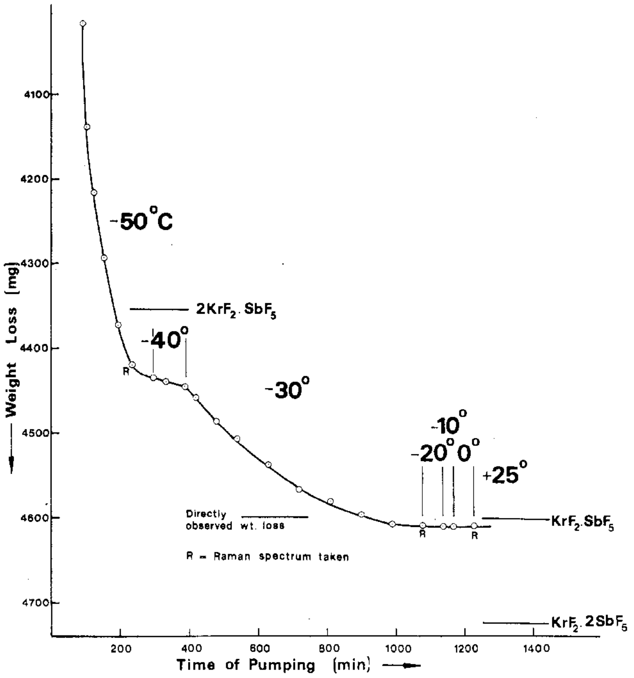

Figure 1. Weight loss vs. time of pumping curve for the reaction of 4.14 mmol of KrF_2 with 2.02 mmol of SbF_5 in BrF_5 at −40 °C.

Preparation of the Tantalum Pentafluoride Adducts. If the reaction of KrF_2 with TaF_5 in anhydrous hydrogen fluoride is carried out in Kel-F containers at room temperature, vigorous attack and the almost immediate fracture of the containers occurs. TaF_5 is only sparingly soluble in BrF_5 at room temperature but, in the presence of KrF_2, solution is effected easily even at −55 °C. These mixtures can be handled in either Kel-F or well-seasoned glass without attack. However, at room temperature krypton and fluorine are rapidly liberated and decomposition is detectable even at −30 °C. In spite of these difficulties we have found that tantalum pentafluoride adducts of KrF_2 can be isolated and characterized provided that temperature conditions are carefully controlled.

$KrF_2{\cdot}TaF_5$ can be obtained by the reaction of TaF_5 with excess of KrF_2 in BrF_5 at −55 °C. In a typical experiment 3.78 mmol of KrF_2 was condensed onto 1.29 mmol of TaF_5 in BrF_5 (2.775 g). The mixture was held at −55 °C for 60 min and then the weight loss vs. time of pumping curve was recorded (Figure 2). Raman spectra of the frozen-solution mixture, recorded during the first 500 min, showed that most of the solvent is removed before the excess of KrF_2 leaves the reaction mixture. Peaks at 595 and 571 cm^{-1} may be assigned to the presence of $[Kr_2F_3]^+$ in solution,[1b] but no evidence of a point of inflection at the 2:1 composition could be found, and the peaks disappear sometime before the 1:1 stoichiometry is reached. Peaks which can be correlated with $KrF_2{\cdot}TaF_5$ (and smaller amounts of $[KrF_2{\cdot}KrF]^+[Ta_2F_{11}]^-$) are also evident. The $KrF_2{\cdot}TaF_5$ finally remaining is stable under a dynamic vacuum at −45 °C but decomposes above this temperature to KrF_2 and TaF_5. No changes are observed in the slope of the decomposition curve (except for those caused by changes in the ambient temperature) and the almost constant slope at −35 °C is indicative of a significant dissociation pressure of the adduct at that temperature. However, Raman spectra of the reaction mixture at various times during the decomposition (see Figure 2) indicate that decomposition

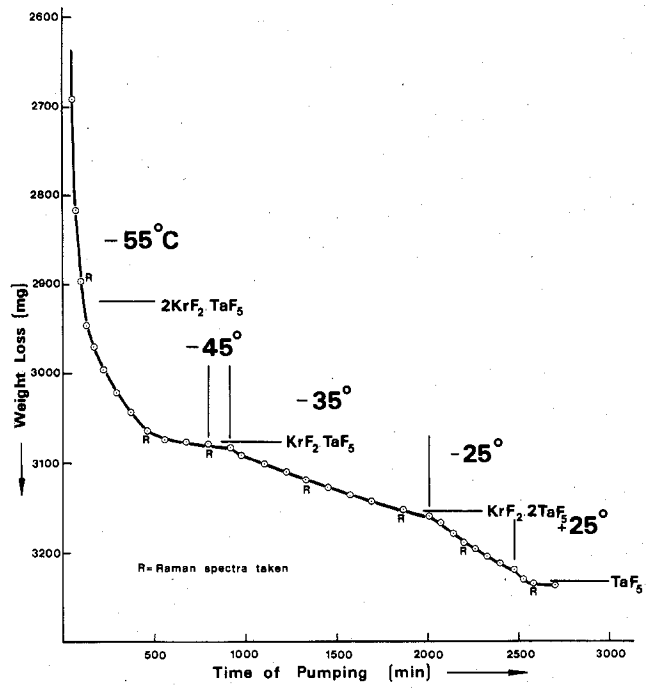

Figure 2. Weight loss vs. time of pumping curve for the reaction of 3.78 mmol of KrF_2 with 1.29 mmol of TaF_5 in BrF_5 at −55 °C.

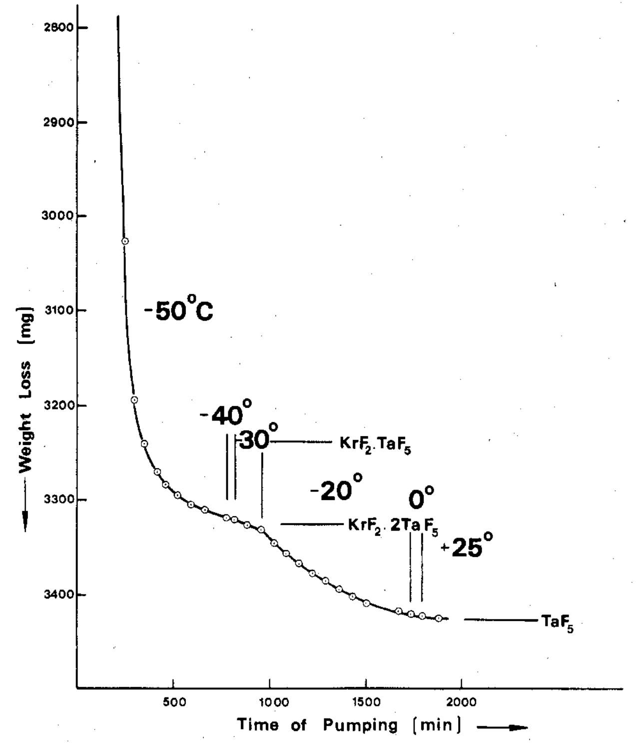

Figure 3. Weight loss vs. time of pumping curve for the reaction of 6.82 mmol of KrF_2 with 1.55 mmol of TaF_5 in BrF_5 at −30 °C.

proceeds via the intermediate $KrF_2 \cdot 2TaF_5$.

$KrF_2 \cdot 2TaF_5$ can be isolated from the solution after excess of KrF_2 has been allowed to react with TaF_5 in BrF_5 at −30 °C for 1 h. The mixture was quenched and the weight loss vs. time of pumping curve was recorded (Figure 3). The decomposition curve and the Raman spectra observed during the course of the decomposition showed no evidence for the occurrence of $KrF_2 \cdot TaF_5$ intermediate in this case. This suggests that at the reaction temperature no $KrF_2 \cdot TaF_5$ adduct is formed. This is in accord with our previous observation that $KrF_2 \cdot TaF_5$ is decomposed at temperatures above −45 °C.

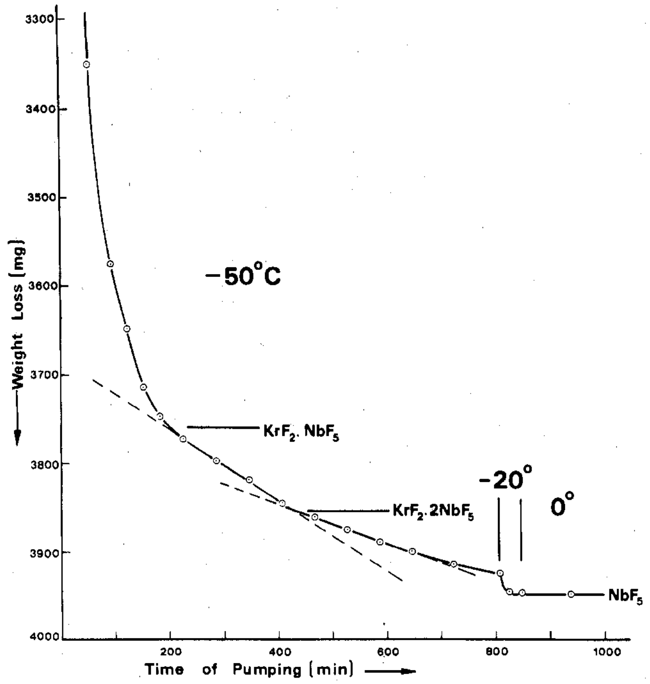

Figure 4. Weight loss vs. time of pumping curve for the reaction of 4.21 mmol of KrF_2 with 1.55 mmol of NbF_5 in BrF_5 at −30 °C.

$KrF_2 \cdot 2TaF_5$, which is white, can be retained under a dynamic vacuum at −50 °C but decomposes slowly above −20 °C to the component molecules.

Preparation of $KrF_2 \cdot 2NbF_5$. We were unable to isolate or find evidence for $KrF_2 \cdot NbF_5$ even in very low-temperature reactions. The only clearly identifiable adduct is $KrF_2 \cdot 2NbF_5$.

In a typical preparation 1.55 mmol of NbF_5 was allowed to react with 4.21 mmol of KrF_2 in BrF_5 (3.454 g) at −40 °C for 20 min. The clear, slightly yellow solution was quenched and the weight loss vs. time of pumping curve was recorded (Figure 4). No evidence for $KrF_2 \cdot NbF_5$ could be found in the Raman spectra of decomposition products but the change in slope after about 170 min of pumping at −50 °C may correspond to decomposition of $[KrF_2 \cdot KrF]^+[Nb_2F_{11}]^-$. However, the Raman spectra recorded throughout the decomposition up to about 430 min do not change appreciably and, therefore, only one compound, $KrF_2 \cdot 2NbF_5$, has been definitely characterized.

The white $KrF_2 \cdot 2NbF_5$ clearly has a considerable dissociation pressure even at −50 °C (in fact it is just slightly lower than the vapor pressure of KrF_2 at that temperature) and the decomposition products are KrF_2 and NbF_5.

General Discussion. The main products of the reactions are formed by the series of schemes outlined in Figure 5. The only room-temperature-stable adducts are $KrF_2 \cdot 2SbF_5$ and $KrF_2 \cdot SbF_5$ and the observed trend in thermal stability under a dynamic vacuum is as follows: $KrF_2 \cdot 2SbF_5 > KrF_2 \cdot SbF_5 > KrF_2 \cdot 2TaF_5 > 2KrF_2 \cdot SbF_5 > KrF_2 \cdot TaF_5 > KrF_2 \cdot 2NbF_5$.

In view of the low thermal stability of $KrF_2 \cdot 2NbF_5$ (which dissociates under a dynamic vacuum even at −50 °C) and the above trends with respect to the antimony and tantalum pentafluoride adducts, it is not surprising that we have been unable to obtain $KrF_2 \cdot NbF_5$.

The fact that $KrF_2 \cdot TaF_5$ is produced at −60 °C but $KrF_2 \cdot 2TaF_5$ is the product of the reaction of KrF_2 and TaF_5 in BrF_5 at −30 °C is in line with the observation (Figures 2 and 5) that $KrF_2 \cdot TaF_5$ decomposes under dynamic vacuum at temperatures in excess of about −35 °C whereas $KrF_2 \cdot 2TaF_5$ is stable under vacuum up to −20 °C.

Vibrational Spectra in the KrF_2–MF_5–BrF_5 (M = Sb, Ta, Nb) Systems. The Raman shift of the symmetrical stretching

1. Large excess of $\mathrm{KrF_2}$ + $[\mathrm{BrF_4}]^+[\mathrm{Sb_2F_{11}}]^-$ (>4:1)

$$\mathrm{KrF_2} + [\mathrm{BrF_4}]^+[\mathrm{Sb_2F_{11}}]^- \xrightarrow[\mathrm{BrF_5}]{-40\ ^\circ\text{C in}}$$

$$\mathrm{2KrF_2\cdot SbF_5(soln)} \xrightarrow[\text{under dynamic vacuum}]{\text{remove solvent at } -50\ ^\circ\text{C}}$$

$$\begin{tikzcd} \mathrm{2KrF_2\cdot SbF_5(cryst)} \arrow[r, "-30\ ^\circ\text{C under}", "\text{dynamic vacuum}"'] & \mathrm{KrF_2\cdot SbF_5} \arrow[d, ">35\ ^\circ\text{C under dynamic vacuum}"'] + \mathrm{KrF_2} \\ & \mathrm{KrF_2}\ (\text{some of which is Kr} + \mathrm{F_2}) + \mathrm{KrF_2\cdot 2SbF_5} \end{tikzcd}$$

2. Excess of $\mathrm{KrF_2}$ + $\mathrm{TaF_5}$ (~3:1)

$$\mathrm{KrF_2 + TaF_5} \xrightarrow[\mathrm{BrF_5}]{-55\ ^\circ\text{C in}}$$

$$\mathrm{KrF_2\cdot TaF_5(soln)} \xrightarrow[\text{under dynamic vacuum}]{\text{remove solvent at } -45\ ^\circ\text{C}}$$

$$\mathrm{KrF_2\cdot TaF_5(cryst)} \xrightarrow[\text{dynamic vacuum}]{-35\ ^\circ\text{C under}}$$

$$(\mathrm{KrF_2\cdot 2TaF_5}\ \text{intermediate}) \xrightarrow[\text{dynamic vacuum}]{-25\ ^\circ\text{C under}} \mathrm{TaF_5 + KrF_2}$$

3. Excess of $\mathrm{KrF_2}$ + $\mathrm{TaF_5}$

$$\mathrm{KrF_2 + TaF_5} \xrightarrow[\mathrm{BrF_5}]{-30\ ^\circ\text{C in}}$$

$$\mathrm{KrF_2\cdot 2TaF_5(soln)} \xrightarrow[\text{dynamic vacuum}]{-50\ ^\circ\text{C under}}$$

$$\mathrm{KrF_2\cdot 2TaF_5(cryst)} \xrightarrow[\text{dynamic vacuum}]{>-20\ ^\circ\text{C under}} \mathrm{TaF_5 + KrF_2}$$

4. Excess of $\mathrm{KrF_2}$ + $\mathrm{NbF_5}$ (>2:1)

$$\mathrm{KrF_2 + NbF_5} \xrightarrow[\mathrm{BrF_5}]{-30\ ^\circ\text{C in}}$$

$$\mathrm{KrF_2\cdot 2NbF_5(soln)} \xrightarrow[\text{dynamic vacuum}]{-50\ ^\circ\text{C under}}$$

$$\mathrm{KrF_2\cdot 2NbF_5(cryst)} \xrightarrow[\text{dynamic vacuum}]{>-50\ ^\circ\text{C under}} \mathrm{NbF_5 + KrF_2}$$

Figure 5. Schemes for the formation of krypton difluoride adducts with $\mathrm{SbF_5}$, $\mathrm{TaF_5}$, and $\mathrm{NbF_5}$.

mode of $\mathrm{KrF_2}$ dissolved in $\mathrm{BrF_5}$ at room temperature appears at 462.5 $\mathrm{cm^{-1}}$ and in the frozen solution (−196 °C) at 475 $\mathrm{cm^{-1}}$. The room-temperature value coincides with ν_1 of solid $\mathrm{KrF_2}$ (462.3 $\mathrm{cm^{-1}}$)[10] which means that the environments of $\mathrm{KrF_2}$ in our solutions and in the solid must be very similar.

The observed Raman and infrared frequencies for the series of adducts are listed in Table I together with our tentative assignments, which are based on the ionic formulations $[\mathrm{Kr_2F_3}]^+[\mathrm{MF_6}]^-$, $[\mathrm{KrF}]^+[\mathrm{MF_6}]^-$, and $[\mathrm{KrF}]^+[\mathrm{M_2F_{11}}]^-$. However, the appearance of Kr···F and M···F (M = Sb, Ta, Nb) bridge stretching modes and the F–Kr···F bending modes in the spectra is indicative of appreciable covalent character, there being a significant contribution to the bonding from fluorine-bridged structures. This is further borne out in the 1:1 adducts by consideration of the spectra associated with the anionic part of the molecule. The spectra can be interpreted by assuming that the compounds are ionic species $[\mathrm{KrF}]^+[\mathrm{MF_6}]^-$ (in which the anion has O_h symmetry). However, for $[\mathrm{KrF}]^+[\mathrm{SbF_6}]^-$ this results in the assignments of peaks in the Raman spectrum as follows: 671 and 647 $\mathrm{cm^{-1}}$ are associated with $\nu_1(\mathrm{a_g})$; 591 $\mathrm{cm^{-1}}$ is associated with $\nu_2(\mathrm{e_g})$; 687 $\mathrm{cm^{-1}}$ is associated with $\nu_3(\mathrm{t_{1u}})$; 270 and 260 $\mathrm{cm^{-1}}$ are associated with $\nu_4(\mathrm{t_{1u}})$; and 294 and 284 $\mathrm{cm^{-1}}$ are associated with $\nu_5(\mathrm{t_{2g}})$. In the infrared spectrum bands at 666 $\mathrm{cm^{-1}}$ have to be assigned to ν_1, and those at 572 $\mathrm{cm^{-1}}$, to ν_2 but no satisfactory assignment for 652 and 630 $\mathrm{cm^{-1}}$ can be made. If, however, the compounds are formulated as fluorine-bridged structures $\mathrm{F{-}Kr^+\cdots F^-{-}MF_5}$, the anion can be regarded as distorted from O_h to C_{4v} symmetry.[9,11] For C_{4v} symmetry 11 normal modes of vibration are expected which are related to the six vibrational modes of the $[\mathrm{MF_6}]^-$ anion of O_h symmetry. In particular the frequencies of the normal modes for the C_{4v} molecule, $\nu_1(\mathrm{a_1})$, $\nu_2(\mathrm{a_1})$, $\nu_8(\mathrm{e})$, $\nu_3(\mathrm{a_1})$, and $\nu_7(\mathrm{b_2})$, should correspond closely to those of the respective normal modes of the O_h molecule. The more satisfactory assignment on the basis of C_{4v} symmetry (see Table I) is an indication of the significant contribution to the bonding from the fluorine-bridged formulation.

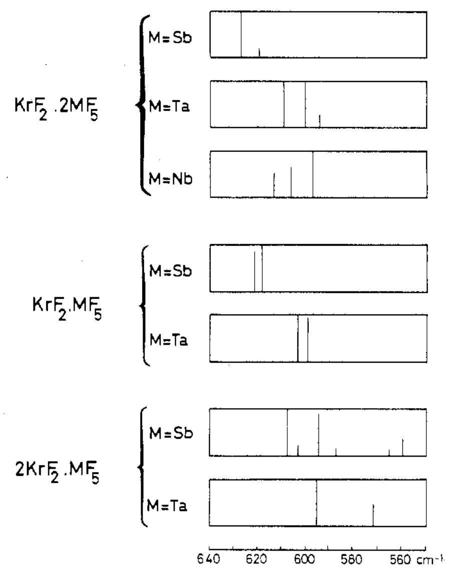

Figure 6. Raman spectra showing stretching frequencies ($\mathrm{cm^{-1}}$) associated with $\mathrm{Kr{-}F^+}$ and $\mathrm{Kr_2F_3^+}$ stretching modes.

Recently we have shown that the stretching frequencies associated with $\nu(\mathrm{Xe{-}F^+})$ for the $\mathrm{XeF_2\cdot 2MF_5}$ and $\mathrm{XeF_2\cdot MF_5}$ (M = Sb, Ta, Nb) adducts decrease in the order $\mathrm{SbF_5 > TaF_5 > NbF_5}$ while those assigned to $\nu(\mathrm{Xe\cdots F})$ increase.[9] There is also a similar correlation between $\mathrm{2XeF_2\cdot SbF_5}$ and $\mathrm{2XeF_2\cdot TaF_5}$.[9] A similar trend is evident in the krypton analogues (Figure 6) except that $[\mathrm{KrF}]^+$ in $[\mathrm{KrF}]^+[\mathrm{Nb_2F_{11}}]^-$ has one band higher in frequency than $[\mathrm{KrF}]^+[\mathrm{Ta_2F_{11}}]^-$. In this case, if a weighted mean is taken, the progression is again evident. This suggests that in each series the antomony adduct is the most ionic and the strength of the fluorine-bridged interaction is increased in the order Sb < Ta < Nb. This is totally in accord with the accepted order of base strengths for the $[\mathrm{SbF_6}]^-$, $[\mathrm{TaF_6}]^-$, and $[\mathrm{NbF_6}]^-$ anions. Comparison of the frequencies of $\nu(\mathrm{Kr{-}F})$ and $\nu(\mathrm{Kr\cdots F})$ for the $[\mathrm{MF_6}]^-$- and $[\mathrm{M_2F_{11}}]^-$-containing adducts of the same metal indicate that the bridging bond in the $[\mathrm{MF_6}]^-$ adduct is weaker in each case (see Table I).

Detailed examination of the Raman spectra observed during the decompositions of adducts containing the most krypton difluoride has revealed a new class of adducts which we have tentatively formulated as $[x\mathrm{KrF_2\cdot KrF}]^+[\mathrm{M_2F_{11}}]^-$. Since we have only observed these species in mixtures with $[\mathrm{KrF}]^+[\mathrm{MF_6}]^-$ and $[\mathrm{KrF}]^+[\mathrm{M_2F_{11}}]^-$ adducts, definitive assignments of all of the peaks is difficult. The principal characteristic of the spectra is a collection of peaks in the 535–575-$\mathrm{cm^{-1}}$ region. These are at higher frequency than the symmetric stretching mode in solid $\mathrm{KrF_2}$ (462.3 $\mathrm{cm^{-1}}$)[10] and may be attributed to $\mathrm{KrF_2}$ loosely associated with one of the anionic–cationic species. Since this association can reasonably be expected to occur at the cation (see below), there should be a partial donation of electron density to the cationic part of the adduct which should be evidenced by a slight drop in the observed frequencies of $\nu(\mathrm{Kr{-}F})$. Table II lists the main assigned

Table I. Observed Infrared (Ir) and Raman (R) Frequencies (cm^{-1}) and Tentative Assignments for $2KrF_2 \cdot MF_5$, $KrF_2 \cdot MF_5$, and $KrF_2 \cdot 2MF_5$ Adducts[c]

		ν(Kr-F)	ν(Kr···F)	δ(F-Kr···F)	MF_6^-	
					ν_1	ν_2
$[Kr_2F_3]^+[SbF_6]^-$ (solid)	R[a]	607 (100) 602.5 (22.5) 595 (93) 587 (11) 565 (15) 559 (40)	334.5 (20) 325.5 (14)	190 (12.5) 186 (10) 181 (10.5) 175 (9)	659 (5) 652 (8.5) 647 (8.5)	576 (6)

		ν(Kr-F)	ν(Kr···F)	δ(F-Kr···F)	$(F\cdots MF_5)^-$								Lattice modes
					ν_4	ν_1	ν_2	ν_5	ν_8	ν_3	ν_{11}	ν_9	
$[KrF]^+[SbF_6]^-$ (solid)	R[b]	621 (85)	348 (2.7)	174 (3.5)	475 (3.5)	671 (41)	647 (12)	591 (4.7)	687 (2.8)	270 (4.2)	260 (3.5)	294 (1.7)	79 (3.7)
		618 (100)	344 (2.7)	166 (4.8)	467 (4.5)							284 (4.1)	55 (8.5)
				149 (2.7)									
	Ir[b]	607 s			~470 m	666 sh	652 br 630 sh	~572 sh					
$[KrF]^+[TaF_6]^-$ (solid)	R[a]	603.5 (100)	343.5 (10)	192 (18)		726 (26)	579 (6.9)	666.6 (10)	626 (19)			296 (2.4)	
		599 (97)	339 (9)	179 (12)								256 (1.6)	
			325 (8.1)										

		ν(Kr-F)	ν(Kr···F)	δ(F-Kr···F)	ν(M···F)	$M_2F_{11}^-$			
$[KrF]^+[Sb_2F_{11}]^-$ (solid)	R[b]	627 (100) 619 (20)	298 (6)? 270 (5) 260 (5)	150 (3)	483 (4.6)	694 (30) 680 (18) 672 (11)	653 (27)	538 (3.8) 524 (8)	228 (5)
	Ir[b]	616 m			482 m	720 sh 686 sh	646 br, vs	580 sh	
$[KrF]^+[Ta_2F_{11}]^-$ (solid)	R[a]	609 (100) 600 (100) 594 (27)?	337 (12)	Not obsd; bad scattering	472 (6)	727 (4) 716 (37) 696 (5)	648 (4) 620 (12)	Not obsd; bad scattering	
$[KrF]^+[Nb_2F_{11}]^-$ (solid)	R[a]	613 (56) 606 (66) 597 (100)	372 (6)	194 (10) 189 (27) 181 (17.3) 167 (9.4)	468 (3) (Coincides with KrF_2)	745 (22) 727 (14) 694 (8) 670 (18)	643 (8)	581 (16)	273 (31) 240

[a] Spectra run at −196 °C. [b] Spectra run at room temperature. [c] Numbers in parentheses are relative intensities.

Table II. Observed Raman Frequencies (cm^{-1}) and Tentative Assignments for $[xKrF_2 \cdot KrF]^+[M_2F_{11}]^-$ (M = Ta, Nb)[a]

	ν(Kr-F)	ν(Kr···F) or $\nu(KrF_2\cdots F)$	δ(F-Kr···F)	ν(M···F)	$\nu(KrF_2)$
$[xKrF_2 \cdot KrF]^+[Ta_2F_{11}]^-$	613 (41)	341 (31) 329 (16.5)	192 (18)[b] 179 (12)[b]	472 (6)[b]	575 (17) 571 (20) 564 (9) 539 (6.7)
$[xKrF_2 \cdot KrF]^+[Nb_2F_{11}]^-$	596 (100)	372 (6)[b] 325 (35)	194 (10)[b] 189 (27)[b] 181 (17.3)[b] 167 (9.4)[b]	468 (3)[b] (Coincides with KrF_2)	571 (52) 541 (9) 535 (14)

[a] x is probably 1. Relative intensities are given in parentheses. All spectra were run at −196 °C. [b] Peaks are coincident with the spectra of the related simpler adduct (see Table I) and assignment, therefore, is dubious.

Raman frequencies for the $[xKrF_2 \cdot KrF]^+[M_2F_{11}]^-$ species.

It has already been pointed out by Gillespie and Schrobilgen,[4] that solid $[Kr_2F_3]^+[SbF_6]^-$ appears to contain an unsymmetrical V-shaped cation (I, Figure 7). It is also possible that it may consist of a mixture of unsymmetrical and symmetrical (I and II, Figure 7) forms. Although it is uncertain how many weakly associated KrF_2 molecules are attached to each $[KrF]^+[M_2F_{11}]^-$ entity in the $[xKrF_2 \cdot KrF]^+[M_2F_{11}]^-$ species, which we have observed, in view of the overall stoichiometry of the mixtures in which they are observed, it seems likely that only one is present. It may, therefore, be possible to regard the $[xKrF_2 \cdot KrF]^+[M_2F_{11}]^-$ adducts as $[Kr_2F_3]^+$ species (i.e., $[xKrF_2 \cdot KrF]^+[M_2F_{11}]^- \equiv [Kr_2F_3]^+[M_2F_{11}]^-$).

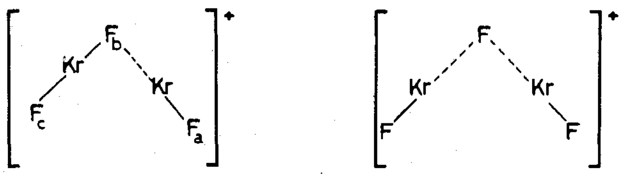

I II

Figure 7. Asymmetric and symmetric $[Kr_2F_3]^+$ cations.

$[Kr_2F_3]^+[SbF_6]^-$ Raman Spectrum. The main shifts in the Raman spectra of the white solids remaining after removal of solvent and KrF_2 from the reactions of KrF_2 with SbF_5 at −40 °C (Table I) can be readily assigned to the $[Kr_2F_3]^+$ cation and the assignment correlates well with that of the xenon difluoride adduct.[8,9] However, additional peaks at 565 and 559 cm^{-1}, which are only 15% and 40% of the height of the main peak associated with ν(Kr-F), also appear in the

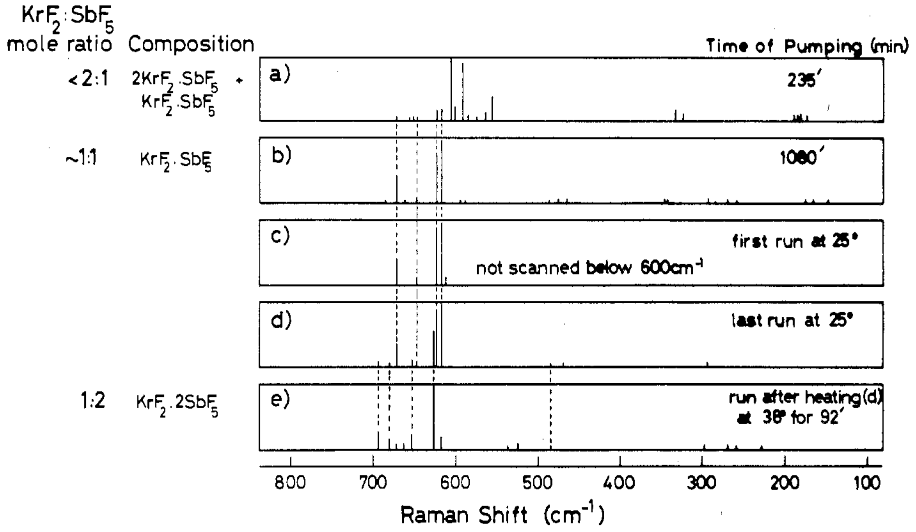

Figure 8. Raman spectra of solids obtained during the vacuum decomposition of the reaction mixture KrF_2–SbF_5–BrF_5. Spectra were run at −196 °C except where otherwise stated.

spectra. The positions of these shifts are intermediate between those associated with ν(Kr–F) in cationic $[KrF]^+$ species and free KrF_2 itself.

In view of the evidence of weak peaks at 623 and 619 cm^{-1}, which seemed to be shifted from the frequencies of bands associated with ν(Kr–F) in $[KrF]^+[SbF_6]^-$ (Table I) we at first assumed[1b] that these, together with the shifts at 565 and 559 cm^{-1}, were associated with $[KrF_2{\cdot}KrF]^+[SbF_6]^-$. Under the conditions in our dynamic experiments, in which species were observed during continuous pumping procedures, this might be expected as the intermediate in the decomposition of a symmetrical V-shaped $[Kr_2F_3]^+$ ion in $[Kr_2F_3]^+[SbF_6]^-$ as it decomposed to KrF_2 and $[KrF]^+[SbF_6]^-$. A second possibility is that the shifts at 565 and 559 cm^{-1} are associated with the $[Kr_2F_3]^+$ cation and that the $2KrF_2{\cdot}SbF_5$ adduct exists as an equilibrium mixture containing both the symmetric and asymmetric cations. A more satisfactory interpretation, however, is that advanced by Gillespie and Schrobilgen[4,12] which suggests that the main peaks in the 585–610-cm^{-1} region and those at 565 and 559 cm^{-1} (557 cm^{-1} in their spectra) should all be assigned to an asymmetric $[Kr_2F_3]^+$ cation (I, Figure 7). The Raman spectrum of $[Kr_2F_3]^+[SbF_6]^-$, assigned on this basis is shown in Table I. A single-crystal x-ray diffraction study could unambiguously confirm this interpretation and will permit detailed comparison with the symmetrical $[Xe_2F_3]^+$ cation.

Raman Spectra of Products Obtained during the Vacuum Decomposition of the KrF_2–SbF_5–BrF_5 Reaction Mixture (See Figure 1). The Raman spectrum recorded during the preparation and decomposition of a $2KrF_2{\cdot}SbF_5$ sample prepared from 4.14 mmol of KrF_2 and 2.02 mmol of SbF_5 is shown in Figure 8. After 235 min of pumping the spectrum, run at −196 °C, indicates that the main constituent is $[Kr_2F_3]^+[SbF_6]^-$. However, additional weaker shifts at 623 and 619 cm^{-1} are very close to the values expected for $\nu(KrF^+)$ in $[KrF]^+[SbF_6]^-$ and that at 671 cm^{-1} coincides with ν_1 of $[SbF_6]^-$ in $[KrF]^+[SbF_6]^-$. The conclusion is, therefore, that after 235 min of pumping, a mixture of $[Kr_2F_3]^+[SbF_6]^-$ and $[KrF]^+[SbF_6]^-$ remains.

It is interesting to note that the spectrum was taken before the point of inflection associated with the composition $2KrF_2{\cdot}SbF_5$ was reached and yet the decomposition curve at −40 °C (Figure 1) shows a greater weight loss than is anticipated for this composition. These observations suggest that, in the presence of low excesses of KrF_2 (starting mole ratio $KrF_2{:}SbF_5$ = 2.09:1.00), an equilibrium such as $Kr_2F_3^+SbF_6^- \rightleftharpoons [KrF]^+[SbF_6]^- + KrF_2$ may occur in the BrF_5 solution. The equilibrium will be pushed to the right by the slow removal of the KrF_2 under the dynamic vacuum. This also explains why free KrF_2 is not observed in the Raman spectrum of the solid.

On further pumping at −30 to 0 °C peaks characteristic for $[KrF]^+[SbF_6]^-$ grow in. Those assigned to $[Kr_2F_3]^+$ disappear and there is a slight shift in the frequencies associated with ν(Kr–F) from 623 and 619 to 621 and 618 cm^{-1}. The spectrum after 1080 min of pumping is interpreted as being essentially pure $KrF_2{\cdot}SbF_5$ (Table I) and the weight loss vs. time of pumping curve confirms the 1:1 stoichiometry (Figure 1).

If samples of $KrF_2{\cdot}SbF_5$ are scanned repeatedly at room temperature, the heat generated by the laser beam causes decomposition of the small area of material under investigation and peaks attributable to $KrF_2{\cdot}2SbF_5$ grow in (see c and d of Figure 8). If $KrF_2{\cdot}SbF_5$ is heated at 38 °C under dynamic vacuum, it is slowly converted to $KrF_2{\cdot}2SbF_5$ (see e of Figure 8).

Raman Spectra of KrF_2–TaF_5–BrF_5 Mixtures. Spectra of Products during the Vacuum Decomposition of the KrF_2–TaF_5–BrF_5 Reaction Mixture. Raman spectra of frozen solutions containing excess of KrF_2 with TaF_5 in BrF_5 exhibit shifts at 477 (72) cm^{-1} due to undissociated KrF_2. There are also bands at 699 (36) and 579.5 (14) cm^{-1} which are due to the ν_1 and ν_2 modes of $[TaF_6]^-$ or related species, while that at 603 (17) cm^{-1} is almost certainly due to $[KrF]^+$ in $[KrF]^+[TaF_6]^-$ (see Table I). The expected related shift at 599 cm^{-1} is not observed but may be obscured by the intense band at 595 (60) cm^{-1} which, together with that at 571 (30) cm^{-1}, is almost certainly due to $[Kr_2F_3]^+$. It appears, therefore, that some of the shifts in the Raman spectra of BrF_5 solutions containing excesses of KrF_2 with TaF_5 can be assigned to $[Kr_2F_3]^+[TaF_6]^-$(solv) as follows: ν(Kr–F) 595 (100), 571 (50); $\nu_1(TaF_6^-)$ 699 (60); $\nu_2(TaF_6^-)$ 579.5 (23) (intensities are scaled so that the most intense peak has a value of 100).

In experiments where mixtures were pumped at −55 °C until most of the BrF_5 solvent was removed, Raman spectra of the residual solids did not exhibit strong features at 595 cm^{-1}.

The Raman spectra of the solids isolated from the reaction of 3.78 mmol of KrF_2 and 1.29 mmol of TaF_5 in BrF_5 at −55 °C are shown in Figure 9. After 104 min of pumping at −55 °C the spectrum consists mainly of peaks associated with $[KrF]^+[TaF_6]^-$ together with free KrF_2 and peaks in the 325–345-cm^{-1} region and at 539 (7), 564 (9), 571 (20), 575 (17), and 613 (18) cm^{-1} and four peaks in the 620–690-cm^{-1}

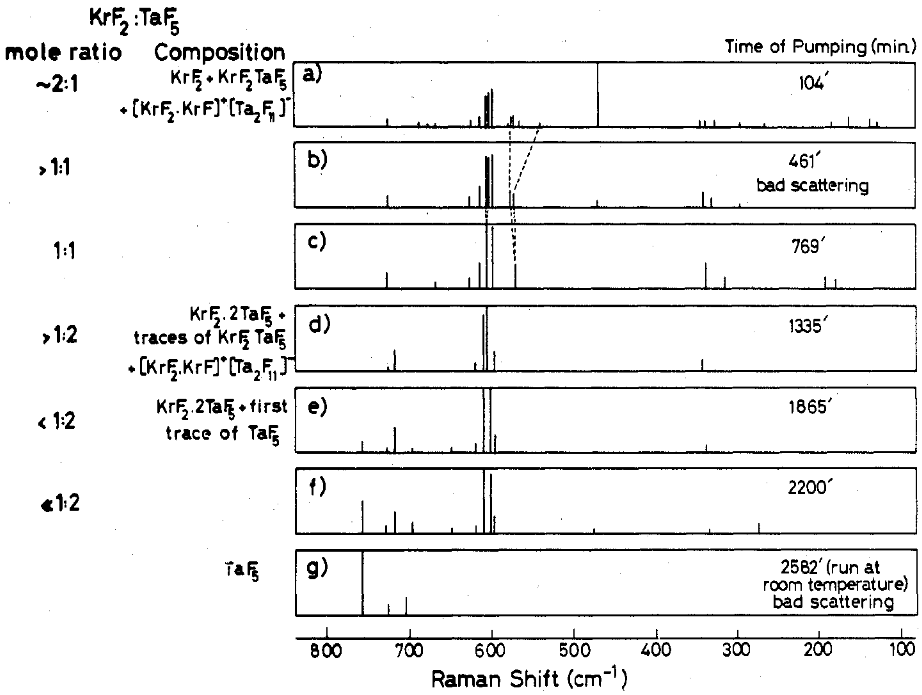

Figure 9. Raman spectra of the solids obtained during the vacuum decomposition of the reaction mixture KrF_2–TaF_5–BrF_5 at −55 °C. Spectra were run at −196 °C except where otherwise stated.

region, all of which we have tentatively attributed to $[xKrF_2{\cdot}KrF]^+[Ta_2F_{11}]^-$. Further pumping reduces the amount of KrF_2 present and after 796 min the shift at 469 cm^{-1} due to free KrF_2 is no longer visible. At the same time the shifts attributable to weakly associated KrF_2 (Table II) collapse first to two shifts at 571 (37) and 576 (33) cm^{-1} and then to a single peak at 569 (42) cm^{-1}. The increase in height of these peaks is paralleled by a similar increase in the height of the band at 613 cm^{-1}. The doublet at 602 (54), 604.5 (46) cm^{-1} associated with $[KrF]^+[TaF_6]^-$ reverts to the, more usual, single shift at 603.5 cm^{-1} (see b and c of Figure 9).

The main features of the Raman spectrum of the compound we have designated $[xKrF_2{\cdot}KrF]^+[Ta_2F_{11}]^-$ are summarized in Table II. The existence and formulation of this entity is not definitive. However, the peak at 613 cm^{-1} associated with ν(Kr–F) is at higher frequency than ν(Kr–F) in any of the tantalum fluoride adducts (see Table I), and the trends evident in Figure 6 suggest, therefore, that this band belongs to a $[KrF]^+$ cation which is associated with $[Ta_2F_{11}]^-$. It seems reasonable to suppose that a proportion of the excess of KrF_2 present is weakly associated with the cation, and we are inclined to formulate this as a transient species $[xKrF_2{\cdot}KrF]^+[Ta_2F_{11}]^-$ rather than as a $[Kr_2F_3]^+$ adduct.

On the assumption that the interpretation above is correct we have interpreted the first spectrum (see a in Figure 9) to mean that initially free KrF_2, $[KrF]^+[TaF_6]^-$, and $[KrF_2{\cdot}KrF]^+[Ta_2F_{11}]^-$ are present in the mixture. The free KrF_2 is removed rather rapidly but, after 769 min of pumping, $[KrF]^+[TaF_6]^-$ contaminated with a smaller proportion of $[KrF_2{\cdot}KrF]^+[Ta_2F_{11}]^-$ remains. The Raman spectra of these two materials seem to disappear from the reaction mixture at about the same time, which indicates that they are of comparable stability.

After 1330 min of pumping almost all evidence of $[KrF]^+[TaF_6]^-$ and $[KrF_2{\cdot}KrF]^+[Ta_2F_{11}]^-$ disappears. The main evidence for this latter compound in the mixture is the persistence of the band at 341 (18) cm^{-1} which does not coincide with any shifts attributable to ν(Kr...F) in $[KrF]^+[Ta_2F_{11}]^-$ and, in any case, is too strong. The principal constituent in the mixture is clearly $[KrF]^+[Ta_2F_{11}]^-$. Small differences in the recorded frequencies and intensities of the observed shifts associated with ν(Kr–F) (609 (89), 601.9 (100), and 595.7 (31) cm^{-1}; c.f. Table I) may not be significant or may be due to the presence of residual $[KrF]^+[TaF_6]^-$ and $[KrF_2{\cdot}KrF]^+[Ta_2F_{11}]^-$. However, after 1865 min of pumping the spectrum of $[KrF]^+[Ta_2F_{11}]^-$ is quite clear and superimposed on it is the first evidence of free TaF_5 (757.5 (14) cm^{-1}). This continues to grow in as pumping continues, and after 2200 min of pumping the peak height is 50% of that of the shifts associated with ν(Kr–F). After 2582 min of pumping most evidence of krypton-containing adducts disappears and the spectrum is essentially that of free TaF_5.

Raman Spectra of Products during Vacuum Decomposition of the KrF_2–NbF_5–BrF_5 Reaction Mixture (See Figure 4). In this case the spectra in the 520–620-cm^{-1} region are essentially consistent throughout the pumping procedure as shown in Figure 10. The intense shift at 476 (145) cm^{-1} in the spectrum run after 77 min of pumping is not coincident with that expected for free KrF_2 and is almost certainly due to the presence of the $KrF_2{\cdot}BrF_5$ molecular adduct. After 192 min the peak is totally absent but a weak band at 468 cm^{-1} is suggestive of small amounts of KrF_2 being still present. The first evidence of free NbF_5 appears in the form of the 773 (5) cm^{-1} peak after 562 min of pumping and this grows in at the expense of the krypton adducts until, after 1920 min only NbF_5 remains (see Figure 10).

Most of the remaining peaks in the spectra can be reasonably assigned on the basis of the formulation $[KrF]^+$-$[Nb_2F_{11}]^-$ (see Table I), but those at 571, ~537, and 322 cm^{-1} cannot. In the KrF_2–SbF_5–BrF_5 system we observed a group of similar peaks (576, 565, 559, 334, and 325 cm^{-1}) which were tentatively assigned to the stretching and bridging vibrations of $[Kr_2F_3]^+$ (or KrF_2 loosely bound to KrF^+). The total absence of any shift which could be assigned to octahedral $[NbF_6]^-$ rules out the presence of an analogous adduct but the spectra and the stoichiometry would allow the existence of $[KrF_2{\cdot}KrF]^+[Nb_2F_{11}]^-$ in the mixture and our assignments (Table II) are consistent with the presence of this species.[9]

Experimental Section

Materials. KrF_2 was prepared by a modified electric discharge method[3] at −183 °C and ~20 mmHg pressure in Pyrex apparatus.

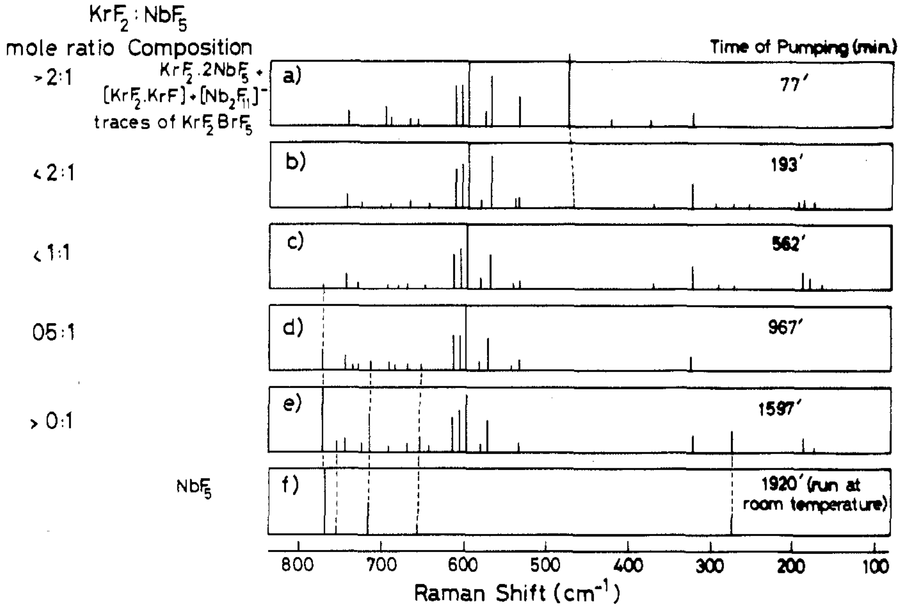

Figure 10. Raman spectra of the solids obtained during the vacuum decomposition of the reaction mixture KrF_2-NbF_5-BrF_5. Spectra were run at −196 °C except where otherwise stated.

The average yield was ~50 mg/h. It was purified by trap to trap sublimation and stored in a preseasoned all-Kel-F container at low temperature.

SbF_5, TaF_5, and NbF_5 were prepared from the elements by pressure fluorination in nickel reactors under static conditions and purified by trap to trap distillation or sublimation under dynamic vacuum.

BrF_5 (Matheson Co., East Rutherford, N.J.) was treated with elemental fluorine at room temperature until colorless and then purified by distillation and stored in an all-Kel-F vessel over KF.

Apparatus. Some reactions were carried out in all-Kel-F test tubes (30-ml volume) or Kel-F 0.75-in. diameter tubes equipped with Kel-F valves. Most preparations were carried out in Pyrex U-tubes (25-ml volume) fitted with an extended bottom of square cross section (7 × 7 mm). The tubes were equipped with Teflon TF2/13 Rotaflo valves and attached to a nickel vacuum line via ground-glass joints and glass-to-metal seals.

Preparation Technique. Reaction tubes were thoroughly seasoned with BrF_5 vapor. Solid pentafluorides were loaded into the reaction tube in a drybox (Lintott Engineering Ltd., Horsham, Essex). SbF_5 was distilled into the reactor under dynamic vacuum. Weights were determined by difference to ±0.2 mg. BrF_5 was distilled onto the pentafluoride, the tube was weighed again, and then KrF_2 was sublimed into the reaction mixture at −196 °C under dynamic vacuum. The amount of KrF_2 was determined by difference on the KrF_2 container.

The reaction mixture was warmed up to the reaction temperature and held there until all of the reactants were in solution. Weight loss vs. time of pumping curves were recorded by attaching a second U-tube to the reaction tube and collecting volatiles at −196 °C. The collection tube was periodically weighed and replaced with another empty collection tube. Thus the amount of volatiles was determined indirectly by differential weighing. Occasionally, Raman spectra of the contents of the reaction tube were recorded at −196 °C. Great care was taken to avoid warming up the reaction tube at any time during the experiment. At the end of each decomposition a direct weight loss was determined by weighing the reaction tube. Very good agreements were obtained; a difference of less than 10 mg was obtained in every experiment after 50 weighings.

Raman Spectra. Raman spectra were recorded using either a Coderg modified PH1 or T800 (with triple monochromator) spectrometer. Exciting radiation was the blue 4880-Å line of a Coherent Radiation Laboratories Model 52 argon ion laser. Usually power of 400 mW was used and the slit aperture was below 2 cm^{-1}. The spectra were recorded at −196 °C with the solids in the reaction tubes partially immersed in liquid nitrogen contained in a transparent Dewar.

Infrared Spectra. Infrared spectra of pulverized solids sandwiched between AgCl plates were recorded using a Perkin-Elmer 225 Grating infrared spectrometer.

X-Ray Diffraction Measurement. X-ray diffraction studies were carried out by the powder technique. Powdered samples were mounted in evacuated Pyrex capillaries and photographed on a Philips 11.64-cm diameter camera with Cu Kα filtered radiation.

Acknowledgment. We are indebted to Mr. Alan Hewitt for supplying purified KrF_2, the SRC for financial support, the Royal Society for an equipment grant, and the Boris Kidrič Foundation for a fellowship to B.F.

Registry No. $[Kr_2F_3]^+[SbF_6]^-$, 52721-22-9; $[KrF]^+[SbF_6]^-$, 58815-70-6; $[KrF]^+[TaF_6]^-$, 58815-71-7; $[KrF]^+[Sb_2F_{11}]^-$, 39578-36-4; $[KrF]^+[Ta_2F_{11}]^-$, 58815-72-8; $[KrF]^+[Nb_2F_{11}]^-$, 58815-73-9; $[Kr_2F_3{}^+][Ta_2F_{11}]^-$, 58815-74-0; $[Kr_2F_3]^+[Nb_2F_{11}]^-$, 58815-75-1; KrF_2, 13773-81-4; $[BrF_4]^+[Sb_2F_{11}]^-$, 29303-54-6; TaF_5, 7783-71-3; NbF_5, 7783-68-8; SbF_5, 7783-70-2.

References and Notes

(1) Some preliminary information has already been published: (a) B. Frlec and J. H. Holloway, *J. Chem. Soc., Chem. Commun.*, 370 (1973); (b) B. Frlec and J. H. Holloway, *ibid.*, 89 (1974).
(2) On leave from Jožef Stefan Institute, University of Ljubljana, Ljubljana, Yugoslavia.
(3) F. Schreiner, J. G. Malm, and J. C. Hindman, *J. Am. Chem. Soc.*, **87**, 25 (1965).
(4) R. J. Gillespie and G. J. Schrobilgen, *J. Chem. Soc., Chem. Commun.*, 90 (1974).
(5) (a) H. Selig and R. D. Peacock, *J. Am. Chem. Soc.*, **86**, 3895 (1964); (b) D. E. McKee, C. J. Adams, A. Zalkin, and N. Bartlett, *J. Chem. Soc., Chem. Commun.*, 26 (1973).
(6) V. N. Prusakov and V. B. Sokolov, *At. Energ.*, **31**, 259 (1971).
(7) V. N. Prusakov and V. B. Sokolov, *Zh. Fiz. Khim.*, **45**, 2950 (1971).
(8) F. O. Sladky, P. A. Bulliner, N. Bartlett, B. G. DeBoer, and A. Zalkin, *Chem. Commun.*, 1048 (1968).
(9) B. Frlec and J. H. Holloway, *J. Chem. Soc., Dalton Trans.*, 535 (1975).
(10) H. H. Claassen, G. L. Goodman, J. G. Malm, and F. Schreiner, *J. Chem. Phys.*, **42**, 1229 (1965).
(11) G. J. Schrobilgen, Ph.D. Thesis, McMaster University, 1973; R. J. Gillespie and G. J. Schrobilgen, *Inorg. Chem.*, in press; R. J. Gillespie, B. Landa, and G. J. Schrobilgen, *ibid.*, in press.
(12) R. J. Gillespie and G. J. Schrobilgen, *Inorg. Chem.*, **15**, 22 (1976).